JACS
JOURNAL OF THE AMERICAN CHEMICAL SOCIETY

Communication

pubs.acs.org/JACS

Accessing Long-Lived Nuclear Spin Order by Isotope-Induced Symmetry Breaking

Michael C. D. Tayler*,‡ and Malcolm H. Levitt

School of Chemistry, Southampton University, SO17 1BJ Southampton, U.K.

Supporting Information

ABSTRACT: Nuclear singlet states are nonmagnetic states of nuclear spin-1/2 pairs that may exhibit lifetimes much slower than the relaxation of the component spins in isolation. This feature makes them attractive vehicles for conveying nuclear hyperpolarization in NMR spectroscopy and magnetic resonance imaging experiments and for reducing signal losses in other NMR experiments caused by undesirably fast nuclear spin relaxation. Here we show access to $^{13}C_2$ singlet states in a symmetrical oxalate molecule by substituting one or more ^{16}O nuclei by the stable nonmagnetic isotope ^{18}O. The singlet relaxation time of the $^{13}C_2$ pair in [1-^{18}O,$^{13}C_2$]-oxalate is 2−3 times longer than the spin−lattice relaxation time T_1.

One of the most promising recent developments in NMR spectroscopy and magnetic resonance imaging (MRI) concerns the development of nuclear hyperpolarization methods, which provide access to substances exhibiting order-of-unity nuclear spin polarization under ambient conditions. Hyperpolarized substances provide NMR signals that can be more than 10^4 times stronger than materials in ordinary thermal equilibrium.[1−3] This enormous enhancement in signal strength has opened up new classes of NMR experiments. One prominent example is the imaging of metabolism *in vivo*, allowing the detection and assessment of cancer.[4,5]

A hyperpolarized material is far from thermal equilibrium. The enhanced nuclear spin order typically decays in a near-exponential process with a time constant T_1, called the spin−lattice or longitudinal relaxation time. In favorable cases this time constant may be as long as 1 min, but in many cases it is much shorter. The entire NMR or MRI experiment, including transport of the hyperpolarized material, introduction into the subject, transport to the site of interest, and the NMR or MRI procedure, must all be conducted while the spin order remains detectable above the thermal noise of the system. This time span is usually a small multiple of T_1 and strongly constrains the applications of the method.

In principle the hyperpolarization lifetime may be extended by exploiting long-lived nuclear spin states, which are collective states of coupled nuclei exhibiting, in favorable circumstances, greatly extended lifetimes. In the case of two spins-1/2, the long-lived mode of nuclear spin order involves the spin-zero singlet state,[6,7] denoted $(|\alpha\beta\rangle - |\beta\alpha\rangle)2^{-1/2}$, where α and β denote spin angular momentum projections $\pm\hbar/2$ along an external axis. Experiments have demonstrated singlet order lifetimes of more than 20 min,[8−10] and several experiments have demonstrated enhanced spin hyperpolarization lifetimes using singlet order.[11−13]

In most cases, the exploitation of nuclear singlet states requires external intervention to suppress the effect of chemical shifts, which otherwise interconvert the long-lived singlet state and the rapidly relaxing triplet states of the spin pair. Procedures involve the transport of the sample into a region of low magnetic field,[14,15] the application of radio frequency fields,[16,17] or the use of chemical reactions to change the symmetry of the molecule.[12] All of these methods work in certain circumstances but have a variety of practical drawbacks.

One way to avoid these problems is to work with molecules which exhibit *near-magnetic equivalence*.[18,19] This implies that the chemical shifts at the two nuclear sites are very similar, but not identical. A strict condition for near-magnetic equivalence is $|\omega^0\Delta\delta| \ll |2\pi J|$, where $\Delta\delta$ is the difference in chemical shifts, J is the scalar spin−spin coupling, $\omega^0 = -\gamma B^0$ is the resonance frequency of the nuclei in the static magnetic field B^0, and γ is the nuclear gyromagnetic ratio. The most important feature of near-equivalent spin-1/2 pairs is that the long-lived singlet order is maintained *without* any external intervention. This avoids the need for transporting the sample into a low-field region $|B^0| \ll |2\pi J/(\gamma\Delta\delta)|$, applying resonant radio frequency fields for long times, or inducing chemical reactions. The long-lived singlet order in near-equivalent systems may be accessed by applying customized radio frequency pulse sequences which exploit the small but finite chemical shift difference.[18,19] These pulse sequences, denoted M2S (magnetization-to-singlet) and S2M (singlet-to-magnetization), exploit carefully timed spin−echo sequences to transport short-lived magnetization to and from long-lived singlet order.

Near-magnetic equivalence may occur naturally as the result of remote chemical asymmetry in the molecule[10,19] or by weak, long-range J-couplings to other nuclei.[20,21] In the current work we demonstrate a different approach. Near-magnetic equivalence may be induced in an otherwise symmetric molecule by substituting nearby atoms by a different spin-zero isotope of the same element. The change in the atomic mass modifies the vibronic motion of the molecular environment and causes small *isotope shifts* that are usually of the order of parts-per-billion (ppb).[22] These small isotope shifts are sufficient to provide access to long-lived singlet order through the M2S and S2M pulse sequences.

Isotope shifts of ^{13}C induced by ^{18}O substitution are illustrated in Figures 1 and 2. Figure 1a shows natural-

Received: December 19, 2012

dx.doi.org/10.1021/ja312227h | J. Am. Chem. Soc. XXXX, XXX, XXX−XXX

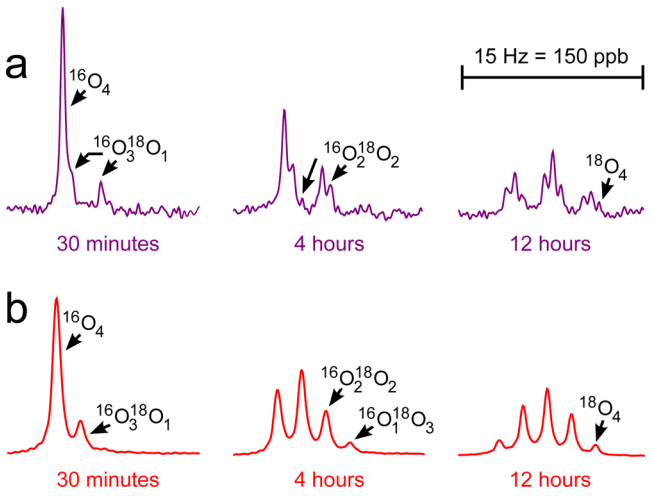

Figure 1. ^{13}C NMR spectra recorded at 9.4 T following dissolution of (a) natural-abundance and (b) 99% $^{13}C_2$-enriched [$^{16}O_4$]-oxalic acid in a 1:1 mixture (by concentration) of $D_2{}^{16}O$:$D_2{}^{18}O$ at 30 °C. The ^{18}O isotopologues formed during acid-catalyzed exchange resolve as separate peaks, due to the ^{18}O isotope shift. The width of each displayed region is 0.15 ppm (15 Hz), centered at 162.02 ppm (referenced to tetramethylsilane).

abundance ^{13}C NMR spectra of oxalic acid ($(COOH)_2$) dissolved in ^{18}O-enriched water (1:1 $D_2{}^{16}O$:$D_2{}^{18}O$), at 30 °C). Initially, a single ^{13}C NMR line is observed in the spectrum, ($\delta_C \approx 162$ ppm). The natural isotopic abundance of oxygen is ca. 99.8% ^{16}O, 0.2% ^{18}O, and therefore essentially all oxalate starts as the [$^{16}O_4$] isotopologue.[23] At later times, peaks at lower chemical shift appear, as acid-catalyzed $^{18}O/^{16}O$ exchange populates the other isotopologues.[24] No couplings are observed with the hydroxyl protons since these are averaged by rapid chemical exchange.

At equilibrium the ^{13}C spectrum contains nine peaks. This is consistent with the fact there are the nine distinct permutations of ^{16}O and ^{18}O around [$^{13}C_1$] oxalate, each isotopologue being resolved through the isotope shift between ^{16}O and ^{18}O.[25−27] The "triplet of triplets" intensity pattern is consistent with ^{18}O-induced ^{13}C isotope shifts that are additive and depend on the number of chemical bonds separating the ^{18}O and the ^{13}C nuclei. It also implies that the two-bond isotope shift does not show dependence upon the OCCO dihedral angle. As Figure 2a illustrates, substitution over the $^{13}C-O$ bond at the 1:1 ratio

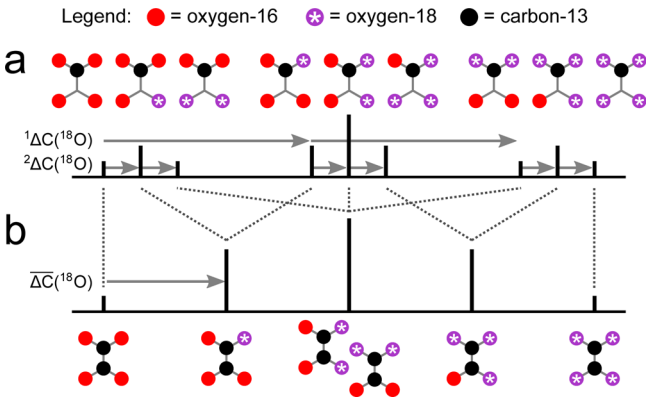

Figure 2. Isotope splitting patterns in the ^{13}C NMR spectra of oxalic acid. The dotted lines show the correlation of ^{18}O isotopomers between the two isotopologues: (a) [$^{13}C_1$] and (b) [$^{13}C_2$].

of ^{16}O to ^{18}O generates a 1:2:1 mixture of [1,1-$^{16}O_2$]-, [1,1-$^{16}O^{18}O$]-, and [1,1-$^{18}O_2$]-oxalate. The ^{13}C resonance frequency in these isotopologues is respectively 0, 1, and 2 times the one-bond isotope shift from that of [$^{16}O_4$]-oxalic acid, therefore giving the appearance of a triplet multiplet pattern. $^{16}O_2$, $^{16}O^{18}O$, and $^{18}O_2$ substitution at the second carbon site splits the apparent "triplet" pattern a second time, this time by the two-bond isotope shift.

The isotope shifts were determined to be $^1\Delta C(^{18}O) = -32 \pm 1$ ppb and $^2\Delta C(^{18}O) = -7 \pm 1$ ppb for the one- and two-bond shifts, respectively. Here we follow the convention[22] where the isotope shift is defined as the change in chemical shift upon substitution of the lighter by the heavier nucleus: $^n\Delta C(^{18}O) = \delta_C(^{18}O) - \delta_C(^{16}O)$, where n denotes the number of chemical bonds between ^{18}O and ^{13}C.

Figure 1b shows the isotopic equilibration of [$^{13}C_2$]-oxalic acid in ^{18}O-water. In this case, the spectrum at equilibrium comprises five peaks with intensity ratio 1:4:6:4:1, spaced equally by the mean of $^1\Delta C(^{18}O)$ and $^2\Delta C(^{18}O)$. This spectral pattern confirms that the $^{13}C_2$ spin pairs remain nearly equivalent, despite the isotope shifts, and that the differences in chemical shift between the nuclear sites are always smaller than the carbon−carbon J coupling. For each $^{13}C_2$ isotopologue, the NMR spectrum contains a single line at the average isotope shift of the spin pair. In [1-$^{18}O_1$,$^{13}C_2$]-oxalic acid, one of the carbons is shifted by $^1\Delta C(^{18}O)$ relative to [$^{16}O_4$,$^{13}C_2$]-oxalic acid, while the other is shifted by $^2\Delta C(^{18}O)$. The average chemical shift is therefore $(^1\Delta C(^{18}O) + {}^2\Delta C(^{18}O))/2$. The peaks in the spectrum of [$^{13}C_2$]-oxalic acid correspond to isotopomers with 0, 1, 2, 3, and 4 atoms of ^{18}O, reading left to right (see Figure 2b).

Of the six ^{18}O isotopologues of $^{13}C_2$-oxalate indicated in Figure 2b, three exhibit asymmetric substitution patterns and are suitable for $^{13}C_2$ singlet NMR. These are the [$^{16}O_3$,$^{18}O_1$,$^{13}C_2$]-oxalate and [$^{16}O_1$,$^{18}O_3$,$^{13}C_2$]-oxalate, both of which have a ^{13}C chemical shift difference $|\Delta\delta_C| = (32 - 7) =$ 25 ppb, and the [1,1-$^{16}O_2$;2,2-$^{18}O_2$;$^{13}C_2$]-oxalate, which has $|\Delta\delta_C| = 2*(32 - 7) = 50$ ppb. The ^{13}C peak of the latter isotopologue, however, coincides with that of the symmetric [1,2-$^{16}O_2$;1,2-$^{18}O_2$;$^{13}C_2$]-oxalate (see also Figure 2b), which makes it more difficult to observe cleanly.

In previous work[18,19] we have shown that the zero-quantum transition between the singlet and triplet states $(|\alpha_1\beta_2\rangle \pm |\alpha_1\beta_2\rangle)2^{-1/2}$ of strongly coupled spins can be stimulated using trains of spin echoes, i.e., repetitive sequences of the form $[\tau/2]-180_\phi{}^\circ-[\tau/2]$, where $[\tau/2]$ is a delay of duration $\tau/2$, and $180_\phi{}^\circ$ denotes a resonant radio frequency pulse of flip angle 180° and phase ϕ. The evolution operators associated with the 180° pulse and the two free-evolution delays both commute with the sum z angular momentum operator. The two states evolve in an isolated zero-quantum subspace. The interchange of $(|\alpha_1\beta_2\rangle + |\alpha_1\beta_2\rangle)2^{-1/2}$ and $(|\alpha_1\beta_2\rangle - |\alpha_1\beta_2\rangle)2^{-1/2}$ requires a train of $N = \text{round}[\pi/|2 \arctan(\Delta\nu/J)|]$ synchronized echoes, where the total duration of each spin echo, $\tau_{echo} = \tau + \tau_p$, assuming τ_p as the pulse duration, is set to $\tau_{echo} = 1/2(J^2 + \Delta\nu^2)^{1/2}$ for spin−spin scalar coupling J and chemical shift frequency difference $\Delta\nu = -\gamma_C B^0 \Delta\delta_C/2\pi$.

The J-coupling $J = {}^1J_{CC}$ does not appear in the spectroscopy of ordinary [$^{16}O_4$]-oxalate, where the two ^{13}C sites are magnetically equivalent, and so was not initially known. The magnitude of $^1J_{CC}$ was therefore determined "directly" on the unsymmetrical [$^{16}O_3{}^{18}O_1$]- and [$^{16}O_1{}^{18}O_3$]-oxalates (both with chemical shift difference $\Delta\delta = (32 - 7) = 25$ ppb), done using

dx.doi.org/10.1021/ja312227h | J. Am. Chem. Soc. XXXX, XXX, XXX−XXX

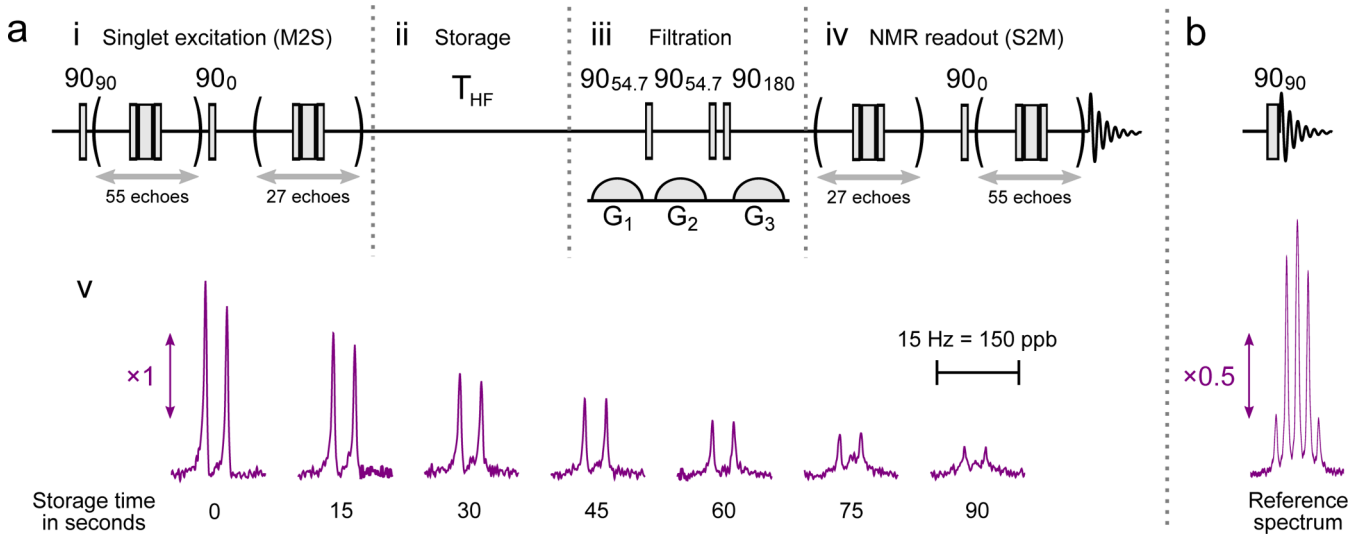

Figure 3. Decay of singlet spin order in [$^{16}O_3$,$^{18}O_1$,$^{13}C_2$]-oxalate and [$^{16}O_1$,$^{18}O_3$,$^{13}C_2$]-oxalate at 30 °C: (a) i–iv, detail of the pulse sequence used, and v, spectra obtained for different waiting times in the high field (single scan); (b) regular 1d ^{13}C spectrum, for comparison (single scan). The displayed regions are centered at 162.02 ppm (referenced to tetramethylsilane). All radio frequency pulses are applied on-resonance.

the procedure described in the Supporting Information. The coupling was determined as $|^1J_{CC}| = 86.9 \pm 0.15$ Hz, corresponding to $\tau_{echo} = 5.75 \pm 0.01$ ms and $N = 55$ at 9.4 T.

To convert longitudinal magnetization of oxalate into singlet spin order, resonant spin echo trains were applied within the M2S pulse sequence shown in Figure 3a. To ensure the longest lifetimes, dissolved paramagnetic oxygen (O_2 gas) was removed from the sample. This was done prior to insertion to the 9.4 T NMR magnet by bubbling the [$^{13}C_2$]-oxalate solution for 15 min with oxygen-free nitrogen gas, then degassing under vacuum.

The mechanism of the M2S sequence has been discussed at length in past work.[18,19] The series of events is briefly as follows: the initial 90° radio frequency pulse and then a train of $N = 55$ spin echoes is applied to convert the equilibrium longitudinal $^{13}C_2$ polarization into singlet–triplet single-quantum coherences. Composite pulses $[90_0180_{90}90_0]_\phi$ are used for the inversions,[28] with the overall phases ϕ cycled through a compensatory four-step list $\phi = (0°,0°,180°,180°)$ in order to minimize rf amplitude and frequency offset errors. The coherences are converted into singlet–triplet zero-quantum coherence by the second 90° radio frequency pulse, whose phase is shifted 90° from the first pulse. A second spin echo train, this time consisting of round$[N/2] = 27$ echoes, finally executes a 90° rotation of the zero-quantum transition to result in a singlet–triplet population difference. Using $\tau_{echo} = 5.75$ ms, the total duration of the conversion is 0.42 s. This duration is short compared to the typical transverse relaxation time T_2 for an isolated $^{13}C_2$ pair in a small molecule, which means that relaxation losses across the M2S conversion are small.

Singlet order was then stored undisturbed in high field for a time $T_{storage}$ (Figure 3a-ii), at the end of which a filtration sequence $[G_1]-90_{54.7°}-[G_2]-90_{54.7°}90_{180°}-[G_3]$ was applied, where G_1, G_2, and G_3 are z pulsed-field-gradients (sine-bell gradient pulses were used, with respective strengths +0.8, −0.8, and −0.8 G cm^{-1} and durations 4.4, 2.4, and 2.0 ms; see Figure 3a-iii). The three gradients induce a rotation of the nuclear spin polarization through an angle dependent on their position within the sample volume. The distribution of rotations is determined by the radio frequency pulses, which are chosen to cause destructive interference of NMR signals passing through spherical tensor operators of ranks one and two.[29] To a good approximation, this leaves only NMR signals passing through rank-zero spin operators, which correspond to singlet nuclear spin order. This is a more general version of the "only parahydrogen spectroscopy" (OPSY) method, often used in parahydrogen-enhanced NMR.[30,31] A similar effect is achieved in low-field singlet NMR by shaking the sample inside a magnetically shielded chamber.[13]

After filtration, singlet order was converted to in-phase transverse magnetization via the S2M sequence (equal to M2S applied in reverse chronological order), with the signal from observable triplet–triplet coherences then acquired (Figure 3a-iv).

Figure 3a-v displays spectra for singlet storage times up to $T_{storage} = 90$ s in high field. These show signals corresponding to [$^{16}O_3{}^{18}O_1$]- and [$^{16}O_1{}^{18}O_3$]-oxalates, while signals from the symmetric oxalates are absent (compare the reference spectrum of the [$^{13}C_2$]-oxalate, Figure 3b). No signal is observed from the unsymmetrical [$^{16}O_2{}^{18}O_2$] isotopologue because the chemical shift difference is exactly twice that for [$^{16}O_3{}^{18}O$] and [$^{16}O{}^{18}O_3$] oxalates. The interchange of the states $(|\alpha\beta\rangle \pm |\beta\alpha\rangle)2^{-1/2}$ for the former isotopologues requires half the number of echoes as for the latter. This implies a 360° rotation (i.e., a refocusing) in the zero-quantum subspace of [$^{16}O_2{}^{18}O_2$], and has the outcome that no singlet order is generated.

Integrals for [$^{16}O_3{}^{18}O_1$]- and [$^{16}O_1{}^{18}O_3$]-oxalate are fit by a monoexponential decay curve $\exp(T_{storage}/T_S)$ to a relaxation time constant $T_S = 55 \pm 5$ s. This decay constant is nearly 3 times longer than the T_1 relaxation time of nuclear triplet spin order, which was measured later at 9.4 T on the same sample by inversion–recovery as 21 ± 0.5 s.

Despite the degassing precautions taken to eliminate dissolved paramagnetic oxygen,[32] the singlet lifetime is much shorter than expected for an isolated pair of ^{13}C spins, which may display lifetimes in excess of 10 min in solution.[10]

This suggests the presence of additional relaxation mechanisms for the $^{13}C_2$ nuclear singlet state. In the present case, it is likely that spin–rotation plays a role,[33] since the moment of inertia of the oxalate anion is small, and the twisted

dx.doi.org/10.1021/ja312227h | J. Am. Chem. Soc. XXXX, XXX, XXX–XXX

equilibrium geometry of the molecule causes the spin−rotation tensors of the two ^{13}C sites to have different orientations. Similar arguments apply to relaxation via chemical shift anisotropy (CSA). Intramolecular dipolar or scalar relaxation may also contribute, as oxalic acid dissolved in water exists mainly in the bound monoanion form ($C_2HO_4^-$) owing to its high acidic strength (pK_a = 1.5 for the diprotic species, 4.5 for the dianion). Longer singlet lifetimes may be expected at lower magnetic field, where CSA is vanishingly small.

In summary, we have shown that the change in ^{13}C chemical shift upon $^{18}O/^{16}O$ substitution generates an asymmetry between the carbon sites in oxalic acid. While in [$^{13}C_2$]-oxalate the isotope-induced asymmetry is 30 times weaker than the spin−spin J coupling, it is sufficiently large that it allows coherent access to the nuclear singlet eigenstate. We expect the concept of isotope-induced symmetry breaking to be useful in singlet NMR of other molecules, plus the spectroscopy of strongly coupled spin pairs in general. Apart from ^{16}O and ^{18}O, shifts from by other isotopic pairs may be exploited, for example ^{32}S and ^{34}S, and ^{35}Cl and ^{37}Cl.

■ ASSOCIATED CONTENT

Supporting Information

Determination of $^1J_{CC}$ coupling in oxalic acid from spin−echo measurements. This material is available free of charge via the Internet at http://pubs.acs.org.

■ AUTHOR INFORMATION

Corresponding Author

m.tayler@science.ru.nl

Present Address

‡Institute for Molecules and Materials/Solid State NMR, Radboud University, Heyendaalseweg 135, 6525 AJ Nijmegen, The Netherlands

Notes

The authors declare no competing financial interest.

■ ACKNOWLEDGMENTS

Support was provided by EPSRC−UK, the European Research Council, and the Leverhulme Trust. The authors are grateful to Neil Wells for use of the 400 MHz NMR spectrometer at Southampton University and also Ilya Kuprov and Giuseppe Pileio for discussions. We acknowledge Judith Schlagnitweit and Norbert Müller for preliminary experiments.

■ REFERENCES

(1) Ardenkjær-Larsen, J. H.; Fridlund, B.; Gram, A.; Hansson, G.; Hansson, L.; Lerche, M. H.; Servin, R.; Thaning, M.; Golman, K. *Proc. Natl. Acad. Sci. U.S.A.* **2003**, *100*, 10158−10163.

(2) Wolber, J.; Ellner, F.; Fridlund, B.; Gram, A.; Jóhannesson, H.; Hansson, G.; Hansson, L. H.; Lerche, M.; Månsson, S.; Servin, R.; Thaning, M.; Golman, K.; Ardenkjær-Larsen, J. H. *NIMA* **2004**, *36*, 173−181.

(3) Griffin, R. G.; Prisner, T. F. *Phys. Chem. Chem. Phys.* **2010**, *12*, 5737−5740.

(4) Albers, M. J.; Bok, R.; Chen, A. P.; Cunningham, C. H.; Zierhut, M. L.; Zhang, V. Y.; Kohler, S. J.; Tropp, J.; Hurd, R. E.; Yen, Y.-F.; Nelson, S. J.; Vigneron, D. B.; Kurhanewicz, J. *Cancer Res.* **2008**, *68*, 8607−8615.

(5) Viale, A.; Aime, S. *Curr. Opin. Chem. Biol.* **2010**, *14*, 90−96.

(6) Levitt, M. H. *Annu. Rev. Phys. Chem.* **2012**, *63*, 89−105.

(7) Levitt, M. H. *Encyclopedia of Magnetic Resonance*; John Wiley & Sons, Ltd.: New York, 2010; Vol. *9*.

(8) Pileio, G.; Carravetta, M.; Hughes, E.; Levitt, M. H. *J. Am. Chem. Soc.* **2008**, *130*, 12582−12583.

(9) Ghosh, R. K.; Kadlecek, S. J.; Ardenkjær-Larsen, J. H.; Pullinger, B. M.; Pileio, G.; Levitt, M. H.; Kuzma, N. N.; Rizi, R. R. *Magn. Reson. Med.* **2011**, *66*, 1177−1180.

(10) Pileio, G.; Hill-Cousins, J.; Mitchell, S.; Kuprov, I.; Brown, L.; Brown, R. C. D.; Levitt, M. H. *J. Am. Chem. Soc.* **2012**, *134*, 17494−17497.

(11) Vasos, P. R.; Comment, A.; Sarkar, R.; Ahuja, P.; Jannin, S.; Ansermet, J. P.; Konter, J. A.; Hautle, P.; van den Brandt, B.; Bodenhausen, G. *Proc. Natl. Acad. Sci. U.S.A.* **2009**, *106*, 18469−18473.

(12) Warren, W. S.; Jenista, E.; Branca, R. T.; Chen, X. *Science* **2009**, *323*, 1711−1714.

(13) Tayler, M. C. D.; Marco-Rius, I.; Kettunen, M. I.; Brindle, K. M.; Levitt, M. H.; Pileio, G. *J. Am. Chem. Soc.* **2012**, *134*, 7668−7671.

(14) Carravetta, M.; Johannessen, O. G.; Levitt, M. H. *Phys. Rev. Lett.* **2004**, *92*, 153003.

(15) Carravetta, M.; Levitt, M. H. *J. Chem. Phys.* **2005**, *122*, 214505.

(16) Carravetta, M.; Levitt, M. H. *J. Am. Chem. Soc.* **2004**, *126*, 6228−6229.

(17) Pileio, G.; Levitt, M. H. *J. Chem. Phys.* **2009**, *130*, 214510.

(18) Pileio, G.; Carravetta, M.; Levitt, M. H. *Proc. Natl. Acad. Sci. U.S.A.* **2010**, *107*, 17135−17139.

(19) Tayler, M. C. D.; Levitt, M. H. *Phys. Chem. Chem. Phys.* **2011**, *13*, 5556−5560.

(20) Feng, Y.; Davis, R. M.; Warren, W. S. *Nat. Phys.* **2012**, *8*, 831−837.

(21) Franzoni, M, B.; Buljubasich, L.; Spiess, H. W.; Münnemann, K. *J. Am. Chem. Soc.* **2012**, *134*, 10393−10396.

(22) Hansen, P. E. *Progr. NMR Spectrosc* **1988**, *20*, 207−255.

(23) *IUPAC Compendium of Chemical Terminology*, 2nd ed.; Blackwell Scientific Publications: Oxford, 1997.

(24) Bunton, C. A.; Carter, J. H.; Llewellyn, D. R.; O'Connor, C.; Odell, A. L.; Yih, S. Y. *J. Chem. Soc.* **1964**, 4615−4622.

(25) Risley, J. M.; van Etten, R. L. *J. Am. Chem. Soc.* **1980**, *102*, 4609−4614.

(26) Risley, J. M.*Encyclopedia of Magnetic Resonance*; John Wiley & Sons, Ltd.: New York.

(27) Moore, R. N.; Diakur, J.; Nakashima, T. T.; McLaren, S. L.; Vederas, J. C. *J. Chem. Soc., Chem. Commun.* **1981**, *155*, 501−502.

(28) Levitt, M. H. *Prog. NMR Spectrosc.* **1986**, *18*, 61−122.

(29) van Beek, J. D.; Carravetta, M.; Antonioli, G. C.; Levitt, M. H. *J. Chem. Phys.* **2005**, *122*, 244510.

(30) Aguilar, J. A.; Adams, R. W.; Duckett, S. B.; Green, G. G. R.; Kandiah, R. *J. Magn. Reson.* **2011**, *208*, 49−57.

(31) Green, R. A.; Adams, R. W.; Duckett, S. B.; Mewis, R. E.; Williamson, D. C.; Green, G. G. R *Prog. Nucl. Magn. Reson. Spectrosc.* **2012**, *67*, 1−48.

(32) Tayler, M. C. D.; Levitt, M. H. *Phys. Chem. Chem. Phys.* **2011**, *13*, 9128−9130.

(33) Pileio, G. *Progr. NMR. Spectrosc* **2010**, *56*, 217−231.

(34) Levitt, M. H. *SpinDynamica*, software for NMR simulation and calculation in Mathematica; www.spindynamica.soton.ac.uk.

(35) *Mathematica*, Version 8.0; Wolfram Research, Inc.: Champaign, IL, 2008.